Geoderma 307 (2017) 189–197

Contents lists available at ScienceDirect

Geoderma

journal homepage: www.elsevier.com/locate/geoderma

Soil water retention, air flow and pore structure characteristics after corn cob biochar application to a tropical sandy loam

E. Amoakwah[a,b,*], K.A. Frimpong[a], D. Okae-Anti[a], E. Arthur[b]

[a] Department of Soil Science, College of Agriculture and Natural Sciences, School of Agriculture, University of Cape Coast, PMB, Cape Coast, Ghana
[b] Department of Agroecology, Faculty of Science and Technology, Arhus University, Blichers Allé 20, P. O Box 50, DK-8830 Tjele, Denmark

ARTICLE INFO

Handling Editor: Morgan Cristine L.S.

ABSTRACT

Soil structure is a key soil physical property that affects soil water balance, gas transport, plant growth and development, and ultimately plant yield. Biochar has received global recognition as a soil amendment with the potential to ameliorate the structure of degraded soils. We investigated how corn cob biochar contributed to changes in soil water retention, air flow by convection and diffusion, and derived soil structure indices in a tropical sandy loam. Intact soil cores were taken from a field experiment that had plots without biochar (CT), and plots each with 10 t ha^{-1} (BC-10), 20 t ha^{-1} without or with phosphate fertilizer (BC-20 and BC-20 + P respectively). Soil water retention was measured within a pF range of 1 to 6.8. Gas transport parameters (air permeability, k_a, and relative gas diffusivity, D_p/D_0) were measured between pF 1.5 and 3.0. Application of 20 t ha^{-1} led to significant increase in soil water retention compared to the CT and BC-10 as a result of increased microporosity (pores < 3 μm) whereas for soil specific surface area, biochar had minimal impact. No significant influence of biochar was observed for k_a and D_p/D_0 for the BC treatments compared to the CT despite the larger values for the two properties in the 20 t ha^{-1} treatments. Although not significant, the diffusion percolation threshold reduced by 34% and 18% in the BC-20 and BC-20 + P treatments, respectively, compared to the CT. Similarly, biochar application reduced the convection percolation threshold by 15 to 85% in the BC-amended soils. The moderate impact of corn cob biochar on soil water retention, and minimal improvements in convective and diffusive gas transport provides an avenue for an environmentally friendly disposal of crop residues, particularly for corn cobs, and structural improvement in tropical sandy loams.

1. Introduction

Soil structural stability, which is defined as the spatial heterogeneity of the different components or characteristics of soil (Dexter, 1988), has enormous effects on plant growth and development, through its effects on soil water balance, and soil workability. Soil structure is a key soil quality factor that can influence crop productivity as it affects storage and movement of soil water, nutrients, and gases within the soil matrix. For instance, soil structure determines the characteristics of water movement in the soil ecosystem, and can thus influence the dissolution and availability of nutrients to growing plants. For agriculture purposes, a healthy soil structure is viewed as that which shows a combination of well-developed soil aggregates and pore systems (Bronick and Lal, 2005), enhancing the exchange of gases between soil and atmosphere. Soil structure also determines the ability of soils to carry out essential ecosystem functions and services such as turnover of organic matter, provision of optimal conditions for microbial activity, and C sequestration (Gregory et al., 2007; Lal and Shukla, 2004). Soil pores occurring within (intra) soil aggregates and between (inter) aggregates serve as pathways for soil water and air movement. The movement of water and gas in the soil profile is influenced not only by the amount of pores and their sizes but also by the pore connectivity and tortuosity (Osozawa, 1998), which is to a large extent related to the geometric characteristics of soil pore structure. Soils with low oxygen diffusivity (below a threshold value of 0.02) restrict root development (Deepagoda et al., 2011), which results in stunted growth and poor yield in crops. The interaction between soil self-organizing processes such as renewal of soil gases and solution by exchange with the environment (Targulian and Krasilnikov, 2007) and management strategies such as incorporation of organic amendments determines the extent of pore structure development (Sun et al., 2013).

Several authors have reported improvements in plant yield following biochar application (Biederman and Harpole, 2013; Blackwell et al., 2009; Jeffery et al., 2014). The improved crop yields found in biochar amended soils is partly attributed to positive improvement in soil physical and hydraulic parameters, such as decreased soil

* Corresponding author at: Department of Agroecology, Faculty of Science and Technology, Arhus University, Blichers Allé 20, P. O Box 50, DK-8830 Tjele, Denmark.
E-mail address: amoakwah.2@osu.edu (E. Amoakwah).

http://dx.doi.org/10.1016/j.geoderma.2017.08.025
Received 21 June 2017; Received in revised form 8 August 2017; Accepted 13 August 2017
0016-7061/

penetration resistance, and bulk density (Busscher et al., 2011) and increased water-holding capacity (Kinney et al., 2012). Also, biochar has high porosity and specific surface area, which can affect the total pore space and gas transport at the soil-atmosphere interface and within the soil ecosystem (Sun et al., 2013). In a study conducted by Obia et al. (2016), application of corn cob biochar at rates of 0.8 to 2.5 w/w% to a tropical sandy soil increased total porosity and available water capacity by 2 to 3% respectively. Studies by Sun et al. (2013) showed that birch wood biochar improved soil pore structure indices such as pore tortuosity and pore organization by enhancing convective gas transport and increasing the ratio of macroporosity to total porosity. Comparatively, biochar has a lighter density than mineral soil, and this property of biochar has been reported by Sun et al. (2015) to significantly increase the total pore spaces of soil. Abel et al. (2013) reported increased total pore volume in the soil medium following the incorporation of 1–5 wt% biochar produced from maize feedstock (mixture of whole plant). Although several studies report beneficial effects of biochar application, detrimental effects may also occur. Most biochars have high pH, with the potential to increase soil pH, and this can potentially increase clay dispersibility due to a dominance of repulsive forces between clay minerals (Roth and Pavan, 1991), and in turn result in decreased aggregation and disruption of soil structure. Kumari et al. (2017) found increased content of water dispersible colloids (WDC) following application of birch wood biochar; an observation they attributed to increased soil pH and decreased electrical conductivity in the biochar-treated soils. Busscher et al. (2010) reported a significant decrease in soil aggregation when biochar produced from pecan shells was applied, whereas Fungo et al. (2017) reported absence of an effect of biochar on soil aggregate stability following application of 2.5 t ha^{-1}eucalyptus wood biochar pyrolyzed at 550 °C to a Typic Kandiudult. Similarly, rice-straw biochar, when applied to an Ultisol, had no effect on soil structural stability (Peng et al., 2011). Undoubtedly, the above enumerated findings on biochar effects on soil aggregate stability are contrasting, thus emphasizing the need to quantify distinct soil and biochar properties for every situation (Khademalrasoul et al., 2014).

Previous studies have reported the effect of biochar application on the volume and architecture of soil pores, however, the mechanisms underlying these changes are yet to be fully understood (Atkinson et al., 2010; Lehmann et al., 2009). Further, for soils of the humid tropics, research on the effects of biochar on gas transport parameters and soil water retention characteristics is relatively limited (Mukherjee and Lal, 2013). Therefore, the objectives of the study were to examine the mechanisms underlying the effect of corn cob biochar on soil water retention, air flow by convection and diffusion, and derived soil structure indices under a series of controlled matric potentials.

2. Materials and methods

2.1. Study area and soil characteristics

The research was conducted at the University of Cape Coast Teaching and Research farm located in the coastal savanna agro ecological zone of Ghana (5°07′N, 1°17′W). The area has two seasons; a rainy season where most rainfall events are recorded between April and October, with June being the wettest month (average rainfall of 327 mm), and a dry season where a long dry spell is recorded between November and March, with March being the hottest month (with a maximum temperature of 31 °C). The area is generally characterized by high rainfall (1400 mm per annum) with mean monthly temperatures ranging from 24 °C to 28 °C. The soil is well-drained sandy loam (18, 9 and 73% by weight of clay silt and sand, respectively) developed on sandstones, shales and conglomerates and classified as a *Haplic Acrisol* (IUSS Working Group WRB, 2015). The chemical properties of the soil in the study area prior to biochar application include the following: 0.93% soil organic carbon, 0.073% total nitrogen, total phosphorus, potassium and magnesium contents were < 0.4, 11.9 and 9.3 mg 100 g^{-1}, respectively, soil pH of 6.1 and an electrical conductivity of 200 μS cm^{-1}.

2.2. Field experimentation and sampling

2.2.1. Biochar properties

The biochar was produced from corn cob feedstock pyrolyzed in a reactor (Lucia stove) with a temperature of 500–550 °C. The biochar produced was sieved to a < 2 mm particle size to obtain a relatively high surface area to improve its reactivity in the soil. The biochar had 85.3% dry matter, 38.8% total carbon, 0.9% total nitrogen, pH of 10.2, 3.31 mg kg^{-1} polycyclic aromatic hydrocarbons, 3150 mg kg^{-1} phosphorus, with Ca^{2+}, Mg^{2+}, K^{+} and Na^{+} of 8690, 4510, 31,800 and 2160 mg kg^{-1}, respectively (Amoakwah et al., 2017).

2.2.2. Field layout

The study adopted the randomized complete block design with thirty-two (32) plots (four treatments with eight replications for each treatment), with each plot measuring 3 m × 6 m (18 m^2). In order to achieve fine tilth, the field was ploughed and harrowed twice, followed by the removal of stubble and weeds. The plots were raised to 15 cm above the natural soil surface to enhance drainage and accommodate access pathways (0.6 m) between plots. Three levels of biochar were used in this study; 10 t ha^{-1} and 20 t ha^{-1}, and 20 t ha^{-1} with P (P-enriched biochar), corresponding to 0, 0.34 and 0.68% respectively. The P-enriched biochar was prepared by mixing 50 kg P_2O_5 ha^{-1} (Triple super phosphate) with 0.68% of biochar. This treatment was included to examine whether pre-treating biochar with P will minimize P fixation by aluminum (Al^{3+}) and hence promote P availability. Investigation into P fixation was not included here since it was not within the scope of this paper. Prior to biochar application, a subsample of the corn cob biochar stock was oven-dried to determine the prevailing water content.

On 7th November 2016, biochar (with and without P fertilizer) was applied by broadcasting on the soil surface of the treatment plots and incorporating it into the soil by plowing to a depth of about 20 cm. To maintain consistency in the treated and untreated plots, all the plots (control and treated) were tilled with a hoe after the biochar application. Hereon, the treatments are denoted by CT, BC-10, BC-20, and BC-20 + P for the 0, 10 t ha^{-1} and 20 t ha^{-1}, and 20 t ha^{-1} with P, respectively. Soil sampling was done on 21st May 2016.

2.3. Soil sampling

Metal core samplers (0.034 m length, 0.061 m in diameter, 100 cm^3 sample volume) were used for intact soil sampling from a depth of 0–20 cm. The sampling for all treatments was done in the center of the plot within rows, avoiding visibly compacted areas. Eight replicate samples were taken for each treatment. At the same locations, disturbed bulk samples were taken for other measurements (texture, organic matter, pH, dry region water retention, etc.)

2.4. Laboratory measurements

2.4.1. Soil texture and organic carbon content

Soil texture was determined by a combination of sieving and hydrometer methods (Gee and Or, 2002). Determination of soil total carbon content was done through the oxidation of carbon to CO_2 at a temperature of 1800 °C with a FLASH 2000 organic elemental analyzer, which was coupled to a thermal conductivity detector (Thermo Fisher Scientific, MA, USA). Since carbonates were absent in the soils, the soil total carbon was considered as soil organic carbon (SOC).

2.4.2. Soil pH and electrical conductivity

Soil pH was determined by mixing 8 ml of air dried soil and 30 ml of deionized water (which corresponds to a soil-water ratio of approximately 1:2.5). Soil pH and EC were subsequently measured by inserting a combined pH and electrical conductivity (EC) electrode into the supernatant (Thomas, 1996).

2.4.3. Soil water retention

2.4.3.1. Wet region measurements. Measurement of wet region water retention was performed in the laboratory at constant temperature of 20 °C. The 32 intact cores were placed in a sand box and saturated with water from underneath, drained and saturated again prior to imposition of suction levels. Suction was applied successively after saturation to establish matric potentials (ψ) of − 10, − 30, − 50, and − 100 cm H_2O (pF 1, 1.5, 1,7, and 2.0; (Schofield, 1935)). Thereafter, samples were moved to a Richard pressure plate apparatus to successively establish matric potentials of − 300, − 500, and − 1000 cm H_2O (corresponding to pF 2.5, 2.7, and 3.0 respectively) according to the methodology described by Dane and Hopmans (2002). At selected potentials, the same soil samples were used for gas transport measurements (described in air permeability and gas diffusion sections below).

2.4.3.2. Dry region measurements. The retention curve from pF 3.8 to 5.0 was obtained with a temperature compensated WP4-T dewpoint Potentiameter (METER Group Inc., Pullman, WA, USA). First, air-dry subsamples from replication plots were oven dried to determine the prevailing water content. Based on the prevailing water content, increasing amounts of water was added to each air-dry subsample to roughly correspond to matric potentials between pF 3.8 and 5.0. A total of eighty (20 from each treatment) subsamples were used for this. To avoid evaporation losses, the moistened soil samples were sealed in Ziploc bags and stored in the refrigerator for 4 weeks to allow equilibration. After the equilibration period, two consecutive soil water potential measurements were taken with the WP4-T. The samples were oven dried at a temperature of 105 °C for 24 h to determine the gravimetric water content.

For the water retention between pF 5.0 and 6.8, a Vapor Sorption Analyzer (METER Group Inc., Pullman, WA, USA) was used. Briefly, 3 g of an air-dry subsample was placed in the instrument and the matric potential and soil mass simultaneously measured. Measurements for each sample were done in duplicate and samples were oven dried afterwards to obtain the gravimetric water content. For further details on the measurement procedure, please consult Arthur et al. (2014) and Likos et al. (2011).

Specific surface area (SA) was estimated from the measured water retention between pF 5.0 and 6.8 using the theoretical Guggenheim-Andersen-de Boer sorption isotherm equation as suggested by Timmermann (2003) and evaluated by Arthur et al. (2017). After obtaining the monolayer water content ($M_{0,}$ kg kg^{-1}) from the GAB modeling of the dry region water retention data, the SA was obtained by the following relation, $SA = M_0NA/w_M$, where N is Avogadro's number (6.02×10^{23} mol^{-1}), A is the area covered by one water molecule (10.8×10^{-20} m^2) and w_M is the molecular weight of water (0.018 kg mol^{-1}).

2.4.4. Air permeability

Air permeability, k_a, was measured by the Forchheimer approach described by Schjønning and Koppelgaard (2017) on cores that were equilibrated at matric potentials of − 30, − 50, − 100, − 300, − 500 and − 1000 cm H_2O. Briefly, four corresponding values of pressure difference, ΔP at values around 5, 2, 1 and 0.5 hPa, were applied across the soil sample placed in an air permeameter, and the resulting air flow, Q was measured. For the purpose of quality control, a 'standard' test (with actual pressure difference, $P_a < 400$ Pa, at target air flow, $Q_t = 3$ ml min^{-1}) was performed prior to soil samples measurement, in two series of steps. First, the system identifies corresponding actual air flow, $Q_{a,}$ and P_a values, where P_a is requested to be within ± 10% of the target pressure difference, $P_t = 5$ hPa. Second, the system finds corresponding values of Q_a and P_a for three additional levels of $\Delta P = \sim 2$, ~ 1, and ~ 0.5 hPa. By measuring at the highest pressure difference of 5 hPa prior to measuring the lower values, the risk that changes in ΔP during a measurement loop will affect water films was curtailed (Schjønning and Koppelgaard, 2017). Darcy's law was then used to calculate k_a in a steady state.

2.4.5. Gas diffusion

The experimental setup that was initially suggested by Taylor (1950) and subsequently improved further by Schjønning (1985) was used for the measurement of gas diffusion (D_p/D_0). Firstly, the gas diffusivity chamber was made oxygen-free by flushing with 100% N_2 gas. The top of the soil core was exposed to the atmosphere to allow atmospheric air to enter into the chamber through the soil sample. Subsequently, O_2 was measured by an electrode mounted on the chamber wall. The O_2 diffusion coefficient in soil (D_p) was calculated as proposed by Rolston and Moldrup (2002). The gas diffusion measurement was done on soil cores already equilibrated at matric potentials (ψ) of − 30, − 50 and − 100, − 300 cm, − 500 and − 1000 cm H_2O. There was a disparity in the time taken for each measurement due to differences in the applied matric potentials, and this difference in the measuring time was considered small enough to neglect the O_2 depletion resulting from microbial consumption (Schjønning et al., 1999).

2.4.6. Bulk density, porosity, and plant available water

After completing the wet region water retention, air permeability and gas diffusion measurements, the samples were oven-dried at 105 °C for 24 h. The weight of each sample was subsequently recorded at each matric potential and after oven drying. The total soil porosity was estimated from the measured bulk density (ρ_b) and a particle density of 2.65 Mg m^{-3}. The volumetric soil water content (θ, m^3 m^{-3}) at each matric potential was taken as the respective difference in weight of the oven-dried samples multiplied by the bulk density (ρ_b). At each matric potential, air-filled porosity (ε, m^3 m^{-3}) was calculated as the difference between the total porosity and volumetric water content (θ, m^3 m^{-3}). The plant available water content (θp, m^3 m^{-3}) was calculated as the difference between the water content at pF 2.5 and pF 4.2.

2.5. Models

The pore size distributions of the soils were derived from the wet region water retention data based on the capillary rise equation by approximating the relationship between Ψ and the equivalent pore diameter (d, μm) (Schjønning, 1992):

$$d = \frac{3000}{\Psi} \tag{1}$$

Pore structure (continuity, complexity, and distribution) was estimated using models based on either gas diffusivity (D_p/D_0) or air permeability (k_a) and (air-filled porosity (ε). The logarithmic form of the exponential model proposed by Marshall (1959) and Millington (1959) was used to relate D_p/D_0 and ε:

$$\log\left(\frac{D_p}{D_o}\right) = \log(m_d) + N_d \log(\varepsilon) \tag{2}$$

where m_d and N_d are fitted parameters. Because of the fact that D_p/D_0 value of 10^{-4} is considered as an indication of zero diffusion through a continuous air-filled pore space (Broecker and Peng, 1974), the ε at that point is considered to be the diffusion percolation threshold, (D_{PT}, m^3 m^{-3})

$$D_{PT} = 10^{-[\log(m_d)+4]/N_d} \tag{3}$$

or an estimate of the volume of pores blocked to exchange of air as reported in previous studies (Schjønning et al., 2002).

Similarly, k_a was related to ε by the logarithmic form of a simple exponential model proposed by Ball et al. (1988):

$$\log(k_a) = \log(m_c) + N_c \log(\varepsilon) \quad (4)$$

where m_c and N_c are fitted model parameters representing soil structural complexity. An estimate of the permeability percolation threshold (C_{PT}, $m^3\ m^{-3}$) was obtained by assuming that a soil with k_a of 1.0 μm^2 is effectively impermeable (Ball et al., 1988).

The applicability of C_{PT} in relation to D_{PT} was assessed for treated and untreated soils. The optimal value of k_a for each of the four soil groups based on the treatments (CT, BC-10, BC-20, and BC-20 + P) was estimated using the relation

$$C_{PT} = 10^{-[\log(m_c)+x]/N_c} \quad (5)$$

where x is the log (k_a) value at which C_{PT} best fit the physically based D_{PT}.

To further assess the differences in pore connectivity and tortuosity after biochar incorporation, the soil pore organization (PO, μm^2) which gives an indication of the pore size distribution was considered for two matric potentials (−100 and −300 cm H_2O) (Groenevelt et al., 1984)

$$PO = \frac{k_a}{\varepsilon} \quad (6)$$

2.6. Data analysis and statistics

Statistical analyses were done using SigmaPlot 11 (Systat Software Inc., San Jose). All the data obtained were checked for normality and homogeneity of variance. Differences between the control and biochar treatments were tested using analyses of variance (ANOVA), after which the Holm-Sidak post-hoc test was used to differentiate between any two given treatments. We used $p < 0.05$ as a criterion for statistical significance of treatment effects, unless otherwise stated. Results are presented as mean ± standard error (SE) in tables and figures.

3. Results

3.1. Soil texture and organic carbon

The particle size distribution and soil organic carbon contents of the treatment plots are presented in Table 1. There was minimal variability within the treatments in terms of soil texture; standard errors for texture ranged from 0.8 to 1.8 for clay, 0.2 to 0.4 for silt, and 0.8 to 1.8 for the sand fraction (Table 1). Among the biochar treatments, only BC-20 treated soils recorded a significant increase of 66% in soil organic carbon (SOC) relative to the CT. The SOC in the BC-10 and BC-20 + P treated soils were statistically similar (Table 1).

3.2. Soil pH and electrical conductivity (EC)

Application of corn cob biochar significantly increased the soil pH by 0.6 and 0.4 units for the BC-20 and BC-20 + P amended soils respectively, relative to the CT. Conversely, incorporation of biochar significantly decrease the EC by 75%, 80% and 79% in the BC-10, BC-20 and BC-20 + P amended plots respectively, compared to the control.

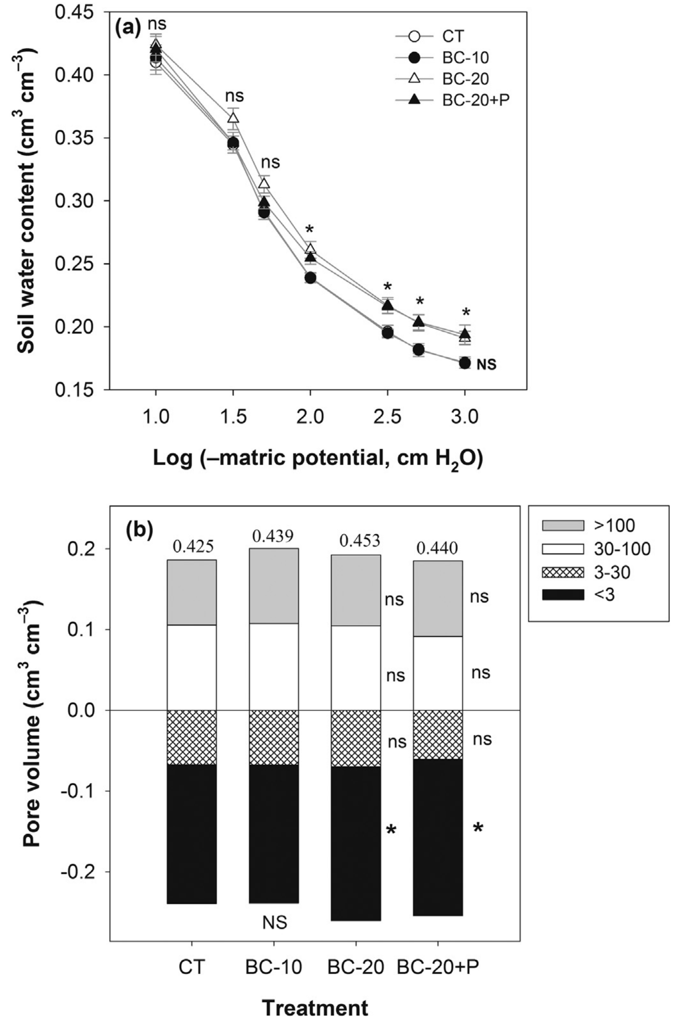

Fig. 1. Corn cob biochar effect on (a) soil water retention and (b) pore size distribution. "NS" indicates no significant difference between BC-10 and CT. Values on top of bars are total pore volumes. "*" indicates significant difference between the water content or pore size class of the BC-20 and BC-20 + P treatment compared to the CT. "ns" indicates no significant difference between the water content or pore size class of the BC treatment and the control. CT, control; BC-10, 20, and 20 + P denote biochar treatments with 10, 20 t ha^{-1}, and 20 t ha^{-1} + 50 kg P_2O_5 t ha^{-1}, respectively.

3.3. Soil bulk density, water retention and specific surface area

Statistically, the bulk density and total porosity in the biochar treated soils were similar to that of the CT (Table 1). The soil water contents found in the various treatments at the different matric potentials are shown in Fig. 1a. There was no significant difference between the biochar treatments and CT when matric potential was ≤ pF 1.5. Between pF 2.0 and 3.0, the BC-20 and BC-20 + P treatments had significantly higher water contents than the BC-10 and CT (Fig. 1a).

Table 1
Effect of corn cob biochar on soil texture, chemical and physical properties.

Treatment	Clay	Silt	Sand	OC	pH	EC	ρ_b	Φ	θ_p
	% by weight				(−)	$\mu S\ cm^{-1}$	$Mg\ m^{-3}$	$m^3\ m^{-3}$	
CT	19 ± 1.8^a	8 ± 0.4^a	73 ± 1.8^a	1.03 ± 0.08^a	5.9 ± 0.1^{bc}	309 ± 46^a	1.52 ± 0.01^a	0.43 ± 0.01^a	0.09 ± 0.01^a
BC-10	18 ± 0.9^a	9 ± 0.3^a	73 ± 1.1^a	1.39 ± 0.18^{ab}	6.2 ± 0.2^{ac}	76 ± 4^b	1.49 ± 0.02^a	0.44 ± 0.02^a	0.10 ± 0.01^a
BC-20	18 ± 0.8^a	8 ± 0.2^a	74 ± 0.8^a	1.71 ± 0.12^b	6.5 ± 0.2^a	61 ± 8^b	1.45 ± 0.03^a	0.45 ± 0.03^a	0.12 ± 0.01^a
BC-20 + P	19 ± 1.6^a	9 ± 0.3^a	72 ± 1.9^a	1.32 ± 0.09^{ab}	6.3 ± 0.1^a	66 ± 8^b	1.49 ± 0.03^a	0.44 ± 0.03^a	0.12 ± 0.01^a

§OC, organic carbon; EC, electrical conductivity, ρ_b, bulk density; Φ, total porosity, θ_p, plant available water content. Different letters indicate that means are significantly different ($p < 0.05$).

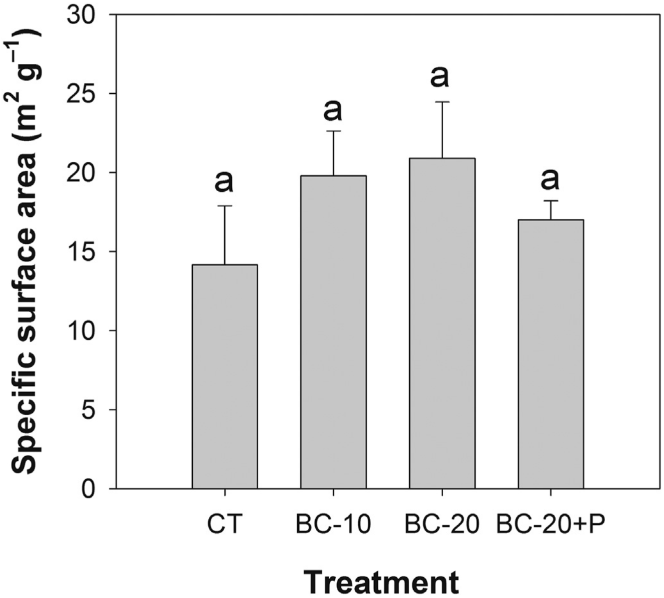

Fig. 2. The soil specific surface area (derived from dry-region soil water retention) as affected by biochar. CT, control; BC-10, 20, and 20 + P denote biochar treatments with 10, 20 t ha^{-1}, and 20 t ha^{-1} + 50 kg P_2O_5 t ha^{-1}, respectively.

Consequently, the biochar treatments showed similar macro- and meso-porosity (pores larger than 30 μm) as the CT (Fig. 1b). Conversely, the BC-20 and BC-20 + P had significantly larger proportions of micropores (pores < 3 μm) than the CT. The BC-10 had a similar trend for both the water retention curve and the pore size fractions compared to the CT. Application of biochar had little impact on the plant available water content (Table 1). Similarly, biochar application did not have any significant effect on the soil specific surface areas (SA) (Fig. 2).

3.4. Air filled porosity and gas transport

Corn cob biochar application had no effect on the relationship between the total air filled porosity (the difference between the total porosity and water content) and the air connected porosity (the pores that are connected in the soil matrix to the atmospheric air). The results showed that all the treatments (CT, BC-10, BC-20 and BC-20 + P) were clustered around the 1:1 line (Fig. 3). The soil's ability to conduct air by diffusion expressed by relative gas diffusivity as a function of matric potential is shown in Fig. 4a. Relative gas diffusivity increased with increasing air filled porosity (decreasing matric potential) for all treatments (Fig. 4). No significant differences were observed between relative gas diffusivity values of the biochar treatments, nor between the biochar treatments and the CT, irrespective of the total porosity of the various treatments (Fig. 4). Soil air permeability increased with decreasing matric potential in all the treatments (Fig. 5a). Though not significant, the BC treatments tended to have larger air permeability values than the CT at matric potentials between 1.5 and 2.0. The $\log_{10}$ of air permeability as a function of $\log_{10}$ air-filled porosity for all treatments is presented in Fig. 5b. For all the treatments, air permeability increased with increasing air-filled porosity. At low air-filled porosities, there was a tendency for larger permeability values for the BC-20 treatments compared to the CT and BC-10 treatments.

3.5. Soil structural indicators

Amendment of the soils with biochar showed no clear trend in soil pore organization (PO) with application rate. For BC-10 and BC-20, PO_{pF2} was about two times that of CT whereas BC-20 + P was identical to the CT. At pF3, PO was numerically similar among all treatments.

Similarly, other indicators of soil structural complexity (N_c and N_d) were not affected significantly by the application of corn cob biochar. Further, biochar incorporation did not have any significant effect on the fraction of the air-filled pores that are inactive in diffusion (denoted by D_{PT}), though there was a reduction of 34% and 18% in D_{PT} in the soils that received the highest biochar application rates (BC-20 and BC-20 + P, respectively) relative to the CT (Table 2). There was an increase of 25% in D_{PT} in the biochar treatment (BC-10) as compared to the CT, even though this increase was not statistically different from the CT soil. Furthermore, corn cob biochar application did not have a significant effect on the convection percolation threshold (C_{PT}). Irrespective of the reduction in C_{PT} by 15%, 85% and 54% in the BC-10, BC-20 and BC-20 + P respectively, as compared to the CT, there was no significant difference in C_{PT} between the biochar treatments and the CT.

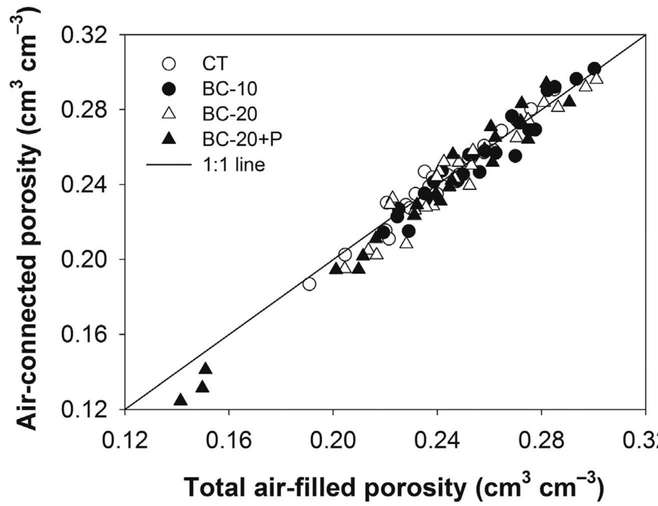

Fig. 3. Relationship between total air-filled porosity (calculated from soil-water retention data) and air-connected porosity measured by a pycnometer. CT, control; BC-10, 20, and 20 + P denote biochar treatments with 10, 20 t ha^{-1}, and 20 t ha^{-1} + 50 kg P_2O_5 t ha^{-1}, respectively.

4. Discussion

4.1. Biochar and soil water retention

4.1.1. Soil density and porosity

Soil bulk density which is considered to be the main driving force of soil physical properties depicts the potential function of the soil with regards to soil aeration, water infiltration, structural support and water and gaseous movement. Results from the study showed that, application of biochar did not change the soil bulk density and total porosity. Previous authors have reported substantial decrease in soil bulk density after the incorporation of different kinds of biochar to different soil types. For example, Arthur and Ahmed (2017) applied 3% w/w of rice straw biochar to a coarse-textured tropical soil and reported a significant (32%) decrease in bulk density, three months after the incorporation of rice straw biochar. This was translated into a 22% and 16% increase in total porosity after 3 months and 15 months of biochar application respectively. Further, in an incubation experiment that lasted for 120 days, Randolph et al. (2017) recorded a significant decrease in bulk density following the application of wood chips and plant residues biochar pyrolyzed at three different pyrolytic temperatures (350 °C, 500 °C and 700 °C) and at an application rate of 2% w/w to sandy clay loam soils. Sun et al. (2015) affirmed that the porous nature and lower density of biochar compared to mineral soil, was responsible for the potential decrease in soil bulk density when they added birch wood biochar pyrolyzed at 500 °C to a sandy loam at application rates of 10 and 50 Mg ha^{-1}. The lack of significant increases in bulk density in our study could be attributed to the low rate of biochar application (a

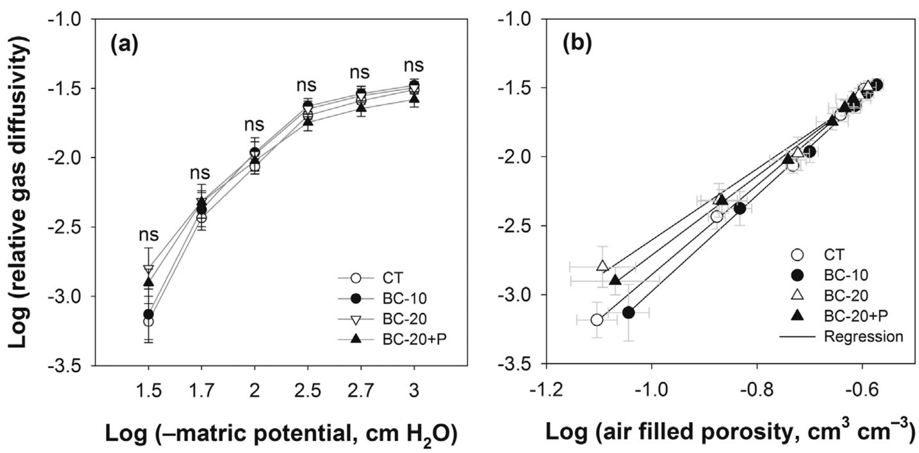

Fig. 4. Relative gas diffusivity (log-scale) as a function of (a) matric potential (in pF units) and (b) total air-filled porosity. "*ns*" indicates no significant difference between treatments for a given matric potential. CT, control; BC-10, 20, and 20 + P denote biochar treatments with 10, 20 t ha^{-1}, and 20 t ha^{-1} + 50 kg P_2O_5 t ha^{-1}, respectively.

maximum of 0.68%) to our soil. The added biochar may not have been enough to substantially dilute the mineral fraction of the soil.

4.1.2. Water retention and pore size distribution

Crop growth, microbial activities and gas exchange dynamics are important processes that are significantly influenced by the ability of the soil to retain water. For the sandy loam in this study, corn cob biochar application at 20 t ha^{-1} showed significant increase in soil water contents at lower matric potentials (pF 2.0–3.0), but at an application rate of 10 t ha^{-1}, no noticeable effect of biochar on soil water retention occurred, possibly due to the low application rate. Precluding all instances of biochar hydrophobicity, an increase in water retained in the soil at a given matric potential after the application of biochar is one of the easily recognizable beneficial effects of biochar. For instance, Randolph et al. (2017) noted a significant increase in water retention after the incorporation of woodchips and plant residues biochars at a rate of 2% w/w to a sandy clay loam. Similarly, Ulyett et al. (2014) reported a significant increase in water retention at a matric potential of − 5 kPa when a deciduous mixed wood biochar pyrolyzed at 600 °C was added to a sandy loam at a rate of 60 t ha^{-1}. The authors ascribed the increase in soil water retention to the intrinsic high surface area of the biochar. A similar observation was made by Głąb et al. (2016) when they applied straw biochar produced at a pyrolytic temperature of 300 °C from miscanthus (*Miscanthus giganteus*) and winter wheat (*Triticum aestivum* L.) at application rates of 0.5%, 1%, 2%, and 4% to a loamy sand. In addition, Karhu et al. (2011) recorded an increase in gravimetric soil water content determined following the incorporation of birch wood biochar pyrolyzed at temperature of 400 °C at an application rate of 9 t ha^{-1} to a silty loam. The authors attributed this increase in water retention to increase in total porosity which led to a corresponding increase in water retention in small pores, and thus increasing the water retention of the soil. The use of pore size distribution to infer soil structure changes induced by different phenomena is becoming common in soil science (Dal Ferro et al., 2014). Different sizes of pores present in the soil medium present distinct and well defined functions in the soil. According to Pires et al. (2017), pores with size (equivalent cylindrical diameter (ECD)) > 50 μm are classified as transmission pores and < 0.50 μm as residual and bonding pores. The transmission pores are responsible for air movement and drainage of excess water, whereas the residual pores are responsible for the retention and diffusion of ions in soil solutions. Lal and Shukla (2004), classified pores with ECD between 0.50 μm and 50 μm as intermediate pores, that are responsible for the release and retention of water against gravity. Biochar at all rates did not produce any significant changes in three of the four pore size fractions considered (3 to < 100 μm) of the sandy loam soils. However, BC-20 and BC-20 + P significantly increased the very fine pores (< 3 μm) compared to the CT. This is important particularly for storage of water for plant uptake. Although plant

Table 2
Biochar effects on soil pore organization (PO) at pF 2 and pF 3, on slopes of log–log plots of relative gas diffusivity and air permeability vs. air-filled porosity (N_d and N_c, respectively) and on the estimates of the diffusion percolation threshold (D_{PT}, m^3 m^{-3}), permeability percolation threshold (C_{PT}, m^3 m^{-3}).

Treatment	PO_{pF2}	PO_{pF3}	N_d	N_c	D_{PT}	C_{PT}
CT	48^{ns}	166^{ns}	3.24^{ns}	3.40^{ns}	0.044^{ns}	0.054^{ns}
BC-10	74	169	3.49	3.17	0.051	0.046
BC-20	88	145	2.58	1.51	0.029	0.008
BC-20 + P	48	144	2.87	2.25	0.036	0.024

"ns" denotes no significant difference among the treatments.

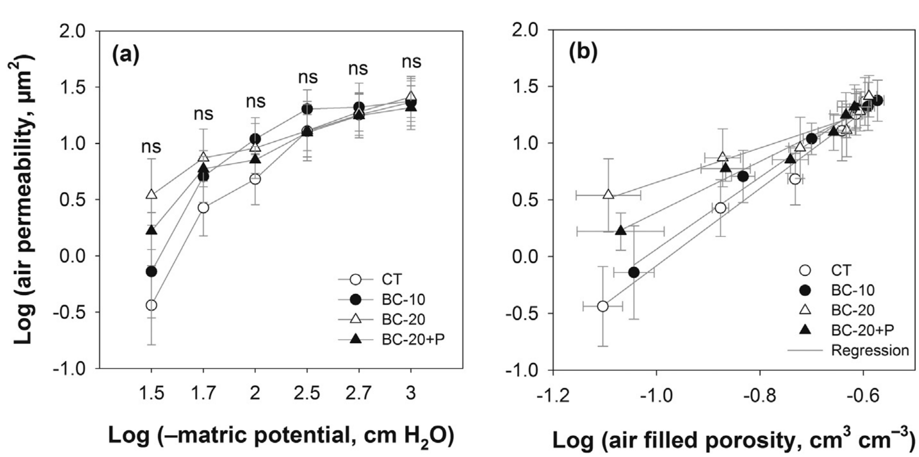

Fig. 5. Soil air permeability (log-scale) as a function of (a) matric potential (in pF units) and (b) total air-filled porosity. "*ns*" indicates no significant difference between treatments for a given matric potential. CT, control; BC-10, 20, and 20 + P denote biochar treatments with 10, 20 t ha^{-1}, and 20 t ha^{-1} + 50 kg P_2O_5 t ha^{-1}, respectively.

available water content (θ_p) was not significantly affected by biochar application, there was a trend of increasing θ_p with increasing biochar rates. For some plants, this marginal increase is particularly important during critical growth periods. Earlier studies that reported significant increases in θ_p were due to an increase in the fraction of smaller pores (0.1–10 μm) and a decrease in the larger pore size fraction. For example, Liu et al. (2016) observed increase in smaller pores (0.1–10 μm) relative to the larger pores (10–1000 μm) when they applied 16 t ha^{-1} of commercial straw biochar pyrolyzed at 500 °C to a loamy soil. Abel et al. (2013) reported an increase in the smaller pore size fractions and a decrease in the larger fractions when they applied biochar pyrolyzed from maize (mix of whole plant) at a temperature of 750 °C and at rates of 1, 2.5 and 5 wt%. Głąb et al. (2016) also found an increased volume of small pores (< 50 μm in diameter) and a decreased volume of larger pores (50–500 μm) when they applied biochar pyrolyzed from miscanthus and winter wheat at 300 °C and at application rates of 0.5, 1, 2 and 4% to loamy sand. In our study, although the BC-20 and BC-20 + P treatments had an increased fraction of small pores, they also had numerically higher fraction of large pores, resulting in marginal effect on the θ_p.

4.1.3. Specific surface area

The soil specific surface area (SA), which was derived from dry-region water retention data (pF 5 to 6.8), is an important property that influences numerous physico-chemical soil properties, and it is determined by the amount of clay and organic matter present in the soil. One of the notable effects of biochar incorporation into soils is an increase in OC, and this has been reported by several authors (e.g., Zhang et al., 2017; Zhu et al., 2017). Results from the study showed that, addition of BC resulted in a significant increase in OC in the BC-20 and BC-20 + P soils. Despite this, there was no significant increase in the SA of the amended soils compared to the control soil possibly due to the relatively short period between the time of biochar application and soil sampling (197 days after biochar application). The SA of soils is controlled primarily by the amount of clay and clay mineralogy (Pennell, 2002) with minimal contribution from soil organic matter for soils with clay content greater than ~20%. As the soil used in the study had clay ~19%, the increases in OC may not be enough to contribute significantly to changes in SA. This explains the contrasting results found in Arthur and Ahmed (2017) where they applied rice straw biochar to a sand-textured soil (clay < 3%) and reported significantly increased SA in the biochar treatments compared to the control.

4.2. Biochar effect on soil air movement and structural complexity

4.2.1. Air movement by conduction and diffusion

Transport of gas in the soil is a very important factor that influences soil aeration and respiration by plant roots. Gas transport characteristics have the potential to affect soil physical quality and crop productivity. Therefore, the quantification of gas transport parameters is important in effective management of physically degraded soils. The ability of soil to conduct air through the pores can be quantified by relative gas diffusivity, D_p/D_o which is driven by concentration gradients, and air permeability, k_a which is driven by pressure gradients. Relative gas diffusivity and air permeability are crucial gas transport parameters that provide insight into gas exchange by diffusion and convection processes, respectively. According to Baral et al. (2016), these two parameters are indicators of soil function, and are important for greenhouse gas emissions. Relative gas diffusivity (D_p/D_0) increased non-linearly with an increase in pF for all the treatments (Fig. 4a). The observed increase in D_p/D_0 as pF increases is attributed to a directly proportional relationship between pF and air-filled porosity. This observation corroborates the findings of Arthur and Ahmed (2017) who reported a larger D_p/D_0 at − 10 kPa than − 3 kPa due to larger air filled porosity at − 10 kPa. Thus, an increase in air filled porosity resulted in a corresponding increase in D_p/D_0 (Fig. 4b). At higher pF values, diffusion of gases in the soil is higher; conversely, higher water contents at lower pF values limit oxygen diffusion (Schjønning et al., 2011).

The D_p/D_0 affects the availability of atmospheric O_2 for intrinsic soil microbes capable of degrading a variety of soil pollutants under aerobic conditions (Davis et al., 2009). The critical D_p/D_0 limits for adequate soil aeration has been reported to be within the range of 0.005–0.02 (Stepniewski, 1981). A study by Schjønning et al. (2006) concluded that the threshold value of D_p/D_0 for adequate diffusion of oxygen in the soil is 0.005. Albeit not significant, at pF 1.7, whereas the CT treatment was in the anaerobic range ($D_p/D_0 < 0.005$), the BC-treated soils had D_p/D_0 values ≥ 0.005. This suggests that, at relatively low pF values, as occurs in wet humid areas, biochar has the potential to facilitate gaseous exchange within the soil ecosystem to enhance soil microbial activity and root respiration. Among the biochar treated soils, BC-10 recorded the highest mean value of D_p/D_0 (0.035) at pF 3. This could be ascribed to the fact that, due to the comparatively high application rates (20 t ha^{-1}), and by virtue of the fact that the biochar were ground (to a particle size of < 2 mm), some of the biochar particles might have filled some of the air-filled pore spaces as the water content decreased. However, the magnitude of the purported infilling of the air-filled pore spaces by the ground biochar in BC-20 and BC-20 + P was not enough to counteract the ability of the soils to facilitate gaseous movement, as D_p/D_0 values of 0.033 and 0.028 (which are above the critical D_p/D_0 value for adequate aeration) were recorded in BC-20 and BC-20 + P respectively.

Air permeability (k_a) controls the movement of air through the soil via convective flow in response to a pressure gradient, and it is a soil physical property that is strongly related to the soil total porosity, pore size distribution, continuity and tortuosity; thus, k_a is sensitive to structural changes as it is directly related to soil structural characteristics. Air permeability increased with increasing pF among the BC treated soils and the CT (Fig. 5a). This is ascribed to the development of more connected pores as the soil dries out at higher pF values. Generally, an increasing trend in k_a was observed in the BC treated soils, particularly at pF < 2.5. This observation contradicts the findings of Arthur and Ahmed (2017) who reported a decrease in k_a 15 months after rice straw biochar application. The authors attributed their observation to an increase in water retention with a subsequent reduction in macropore fraction after the biochar application. A significant decrease in k_a was also reported by Wong et al. (2016), when they applied peanut shell biochar pyrolyzed at 500 °C to clayey soil at application rates of 5, 10 and 15%. The authors attributed this observation to a decreased soil inter-pores at a high biochar application, suggesting that k_a is mainly governed by inter-aggregate pores at low biochar content. The possible reason to our observation is that, the corn cob biochar applied did not significantly increase the water content to warrant the presence of blocked pores. Hence, there was a considerable fraction of the air-filled pores that were relatively active in conducting air in the soil matrix.

4.2.2. Pore structure and gas percolation thresholds

To elucidate the effect of corn cob biochar on soil structure, the soil pore organization (PO) was evaluated to compare the structural complexity between the biochar treated soils and the CT. The PO parameter gives an indication of the structural differences in differently managed soils (Chamindu Deepagoda et al., 2013), as smaller PO values are attributed to more tortuous pore structure (and thus more complex structure), implying an improved pore continuity than large PO values. From the study, PO was computed at two matric potentials (pF 2 and pF 3) at which D_p/D_0 and k_a were measured (Table 2). No significant difference was observed in soil PO between the biochar treated soils and the CT at both matric potentials. At pF 2, no distinct pattern could be seen in PO between the CT and the biochar treated soils. However, PO was lower in the BC-20 and BC-20 + P treatments at pF 3. Comparatively, soil PO computed at pF 2 was lower than that of pF 3. This is probably because at low pF, the length of convection pathway is high due to low pore continuity and an increase in apparent tortuosity.

The diffusion of gases in water has been reported by several authors to be slower than that in air by a factor of 10^4 (Moldrup et al., 2004; Thorbjorn et al., 2008). Based on this premise, Arthur et al. (2013) posited that a relative gas diffusivity value of 10^{-4} may be considered as a threshold for diffusion through connected air-filled pores. Any value below the threshold value implies that diffusion occurs in the water phase. Therefore, it can be inferred that the air-filled porosity at which the D_p/D_0 threshold occurs is the diffusion percolation threshold, denoted by D_{PT}, from Eq. (3). According to Arthur et al. (2013), the D_{PT} value expresses the fraction of air-filled pores that are not active in diffusion due to the fact that these pores are blocked by water or they are embedded in aggregates. Though not statistically significant, the soils treated with BC-20 and BC-20 + P recorded lower D_{PT} values relative to the CT (Table 2). This observation implies that, most of the pores in the BC-20 and BC-20 + P soil were actively involved in diffusive gas transport, giving a further indication that these biochar treated soils may have lower structural complexity than the CT. This assertion is further substantiated by the low PO values obtained at pF 3 for the BC-20 and BC-20 + P soils.

Similar to D_{PT} is the convection percolation threshold C_{PT}, which is suggested by Ball et al. (1988) to exist when air permeability (k_a) = 1.0 μm. On the average, D_{PT} was observed to be higher than C_{PT} in the biochar amended soils. This was not expected considering the diverse pore domains that dictate convective and diffusive gas flows. Comparatively, convective flow preferentially occurs in macropores that are well drained, whereas flow of gas by diffusion takes place in virtually all pores, giving it a higher probability of yielding a lower D_{PT} values than C_{PT}. Our findings contradict the observation made by Masís-Meléndez et al. (2015) who reported lower values in D_{PT} than C_{PT}. This observation from our study may be attributed to a relatively larger water content in the network of arterial pores that directly influence gas diffusion along the axes of the cores in the biochar amended soils, hence, the lower D_{PT} values observed in the BC treatments relative to the C_{PT} values. The relatively lower C_{PT} values observed in the BC treated soils may also be due to an increase in air-filled pore space (drained macropores) that led to a subsequent increase in the interconnected pathways for a convective gas transport in the BC amended soils.

5. Conclusions and recommendations

This study demonstrated that addition of 10 t ha^{-1} and 20 t ha^{-1} of corn cob biochar to a tropical sandy loam has moderate impacts on soil water retention, and no clear effect on air flow by convection and diffusion, and derived soil structure indices. Specifically:

– Larger water contents was observed for the 20 t ha^{-1} biochar treatments relative to the control treatment only for matric potentials larger than pF 2.0; due to an increase in fine pores in the biochar treatments (< 3 μm).
– Corn cob biochar application did not significantly affect the bulk density, total porosity, plant available water and specific surface area of the soil.
– Soil air permeability and gas diffusion as a function of air-filled porosity was not significantly affected by biochar application. Consequently, soil structure complexity was statistically similar for all treatments.

The observations mentioned above were made for corn cob biochar with relatively small application rates and short residence time (197 days) between application and soil sample collection; hence the lack of significant differences in the gas transport and pore structure characteristics. Further and/or complimentary studies with higher biochar application rates and possibly, with different types of biochar and soil types, and over a longer time period are recommended to elucidate general biochar effects on soil functions in tropical ecosystem.

Acknowledgements

We thank Bodil B. Christensen and Michael Koppelgaard for the technical assistance, and to Danida (Ministry of Foreign Affairs of Denmark) for the financial support to the project “Green Cohesive Agricultural Resource Management, WEBSOC”, DFC project no: 13-01AU.

References

Abel, S., Peters, A., Trinks, S., Schonsky, H., Facklam, M., Wessolek, G., 2013. Impact of biochar and hydrochar addition on water retention and water repellency of sandy soil. Geoderma 202–203, 183–191.
Amoakwah, E., Frimpong, K.A., Arthur, E., 2017. Corn cob biochar improves aggregate characteristics of a tropical sandy loam. Soil Sci. Soc. Am. J (Under review).
Arthur, E., Ahmed, F., 2017. Rice straw biochar affects water retention and air movement in a sand-textured tropical soil. Arch, Agron. Soil Sci. 1–13.
Arthur, E., Moldrup, P., Schjønning, P., de Jonge, L.W., 2013. Water retention, gas transport, and pore network complexity during short-term regeneration of soil structure. Soil Sci. Soc. Am. J. 77, 1965–1976.
Arthur, E., Tuller, M., Moldrup, P., Greve, M.H., Knadel, M., de Jonge, L.W., 2017. Applicability of the GAB water vapour sorption model for estimation of soil specific surface area. Eur. J. Soil Sci (under review).
Arthur, E., Tuller, M., Moldrup, P., Wollesen de Jonge, L., 2014. Rapid and fully automated measurement of water vapor sorption isotherms: new opportunities for vadose zone research. Vadose Zone J. 13.
Atkinson, C.J., Fitzgerald, J.D., Hipps, N.A., 2010. Potential mechanisms for achieving agricultural benefits from biochar application to temperate soils: a review. Plant Soil 337 (1), 1–18.
Ball, B.C., O'Sullivan, M.F., Hunter, R., 1988. Gas diffusion, fluid flow and derived pore continuity indices in relation to vehicle traffic and tillage. J. Soil Sci. 39 (3), 327–339.
Baral, K.R., Arthur, E., Olesen, J.E., Petersen, S.O., 2016. Predicting nitrous oxide emissions from manure properties and soil moisture: an incubation experiment. Soil Biol. Biochem. 97, 112–120.
Biederman, L.A., Harpole, W.S., 2013. Biochar and its effects on plant productivity and nutrient cycling: a meta-analysis. GCB Bioenergy 5 (2), 202–214.
Blackwell, P.S., Riethmuller, G., Collins, M., 2009. Biochar application for soils. Chapter 12. In: Lehman, J., Joseph, S. (Eds.), biochar for Environmental Management Science and Technology. 207–226 Earthscan, London.
Broecker, W.S., Peng, T.H., 1974. Gas exchange rates between air and sea1. Tellus 26 (1–2), 21–35.
Bronick, C.J., Lal, R., 2005. Soil structure and management: a review. Geoderma 124 (1–2), 3–22.
Busscher, W.J., Novak, J.M., Ahmedna, M., 2011. Physical effects of organic matter amendment of a southeastern US coastal loamy sand. Soil Sci. 176 (12), 661–667.
Busscher, W.J., Novak, J.M., Evans, D.E., Watts, D.W., Niandou, M.A.S., Ahmedna, M., 2010. Influence of pecan biochar on physical properties of a Norfolk loamy sand. Soil Sci. 175 (1), 10–14.
Chamindu Deepagoda, T.K.K., Arthur, E., Moldrup, P., Hamamoto, S., Kawamoto, K., Komatsu, T., de Jonge, L.W., 2013. Modeling air permeability in variably saturated soil from two natural clay gradients. Soil Sci. Soc. Am. J. 77, 362–371.
Dal Ferro, N., Sartori, L., Simonetti, G., Berti, A., Morari, F., 2014. Soil macro- and microstructure as affected by different tillage systems and their effects on maize root growth. Soil Tillage Res. 140, 55–65.
Dane, J.H., Hopmans, J.W., 2002. Water retention and storage. In: Dane, J.H., Topp, G.C. (Eds.), Methods of Soil Analysis. Part 4. Physical Methods. SSSA Book Series 5. 688–690 SSSA, Madison, WI.
Davis, G.B., Patterson, B.M., Trefry, M.G., 2009. Evidence for instantaneous oxygen-limited biodegradation of petroleum hydrocarbon vapors in the subsurface. Ground Water Monit. Remediat. 29 (1), 126–137.
Deepagoda, T.K.K.C., Moldrup, P., Schjønning, P., Kawamoto, K., Komatsu, T., De Jonge, L.W., 2011. Generalized density-corrected model for gas diffusivity in variably saturated soils. Soil Sci. Soc. Am. J. 75 (4), 1315–1329.
Dexter, A.R., 1988. Advances in characterization of soil structure. Soil Tillage Res. 11 (3), 199–238.
Fungo, B., Lehmann, J., Kalbitz, K., Thionġo, M., Okeyo, I., Tenywa, M., Neufeldt, H., 2017. Aggregate size distribution in a biochar-amended tropical Ultisol under conventional hand-hoe tillage. Soil Tillage Res. 165, 190–197.
Gee, G.W., Or, D., 2002. Particle size analysis. In: Dane, J.H., Topp, G.C. (Eds.), Methods of Soil Analysis. Part 4 - Physical Methods Book Series no. 5. 255–293 Soil Sci. Soc, Madison, WI.
Głąb, T., Palmowska, J., Zaleski, T., Gondek, K., 2016. Effect of biochar application on soil hydrological properties and physical quality of sandy soil. Geoderma 281, 11–20.
Gregory, A.S., Watts, C.W., Whalley, W.R., Kuan, H.L., Griffiths, B.S., Hallett, P.D., Whitmore, A.P., 2007. Physical resilience of soil to field compaction and the interactions with plant growth and microbial community structure. Eur. J. Soil Sci. 58 (6), 1221–1232.
Groenevelt, P.H., Kay, B.D., Grant, C.D., 1984. Physical assessment of a soil with respect to rooting potential. Geoderma 34 (2), 101–114.
IUSS Working Group WRB, 2015. World Reference Base for Soil Resources 2014, Update

2015. International Soil Classification System for Naming Soils and Creating Legends for Soil Maps, World Soil Resources Reports no. 106 FAO, Rome.
Jeffery, S., Verheijen, F.G.A., Bastos, A.C., Van Der Velde, M., 2014. A comment on 'biochar and its effects on plant productivity and nutrient cycling: a meta-analysis': on the importance of accurate reporting in supporting a fast-moving research field with policy implications. GCB Bioenergy 6 (3), 176–179.
Karhu, K., Mattila, T., Bergström, I., Regina, K., 2011. Biochar addition to agricultural soil increased CH4 uptake and water holding capacity - results from a short-term pilot field study. Agric. Ecosyst. Environ. 140 (1–2), 309–313.
Khademalrasoul, A., Naveed, M., Heckrath, G., Kumari, K.G.I.D., de Jonge, L.W., Elsgaard, L., Vogel, H.-J., Iversen, B.V., 2014. Biochar effects on soil aggregate properties under no-till maize. Soil Sci. 179 (6), 273–283.
Kinney, T.J., Masiello, C.A., Dugan, B., Hockaday, W.C., Dean, M.R., Zygourakis, K., Barnes, R.T., 2012. Hydrologic properties of biochars produced at different temperatures. Biomass Bioenergy 41, 34–43.
Kumari, K.G.I.D., Moldrup, P., Paradelo, M., Elsgaard, L., de Jonge, L.W., 2017. Effects of biochar on dispersibility of colloids in agricultural soils. J. Environ. Qual. 46 (1), 143–152.
Lal, R., Shukla, M.K., 2004. Principles of Soil Physics.
Lehmann, J., Czimczik, C., Laird, D., Sohi, S., 2009. Stability of biochar in the soil. chapter 11. In: Lehmann, J., Joseph, S. (Eds.), Biochar for Environmental Management Science and Technology. Earthscan, London, UK, pp. 183–205.
Likos, W., Lu, N., Wenszel, W., 2011. Performance of a Dynamic Dew Point Method for Moisture Isotherms of Clays.
Liu, C., Wang, H., Tang, X., Guan, Z., Reid, B.J., Rajapaksha, A.U., Ok, Y.S., Sun, H., 2016. Biochar increased water holding capacity but accelerated organic carbon leaching from a sloping farmland soil in China. Environ. Sci. Pollut. Res. 23 (2), 995–1006.
Marshall, T.J., 1959. The diffusion of gases through porous media. J. Soil Sci. 10 (1), 79–82.
Masís-Meléndez, F., de Jonge, L.W., Chamindu Deepagoda, T.K.K., Tuller, M., Moldrup, P., 2015. Effects of soil bulk density on gas transport parameters and pore-network properties across a sandy field site. Vadose Zone J. 14.
Millington, R.J., 1959. Gas diffusion in porous media. Science 130 (3367), 100–102.
Moldrup, P., Olesen, T., Yoshikawa, S., Komatsu, T.A., Rolston, D., 2004. Three-porosity Model for Predicting the Gas Diffusion Coefficient in Undisturbed Soil. 68. pp. 750–759.
Mukherjee, A., Lal, R., 2013. Biochar impacts on soil physical properties and greenhouse gas emissions. Agronomy 3 (2), 313.
Obia, A., Mulder, J., Martinsen, V., Cornelissen, G., Børresen, T., 2016. In situ effects of biochar on aggregation, water retention and porosity in light-textured tropical soils. Soil Tillage Res. 155, 35–44.
Osozawa, S., 1998. A simple method for determining the gas diffusion coefficient in soils and its application to soil diagnosis and analysis of gas movement in soil. In: Bulletin of the National Institute of Agro-Environmental Sciences, Ibaraki, Japan No. 15.
Peng, X., Ye, L.L., Wang, C.H., Zhou, H., Sun, B., 2011. Temperature- and duration-dependent rice straw-derived biochar: characteristics and its effects on soil properties of an ultisol in southern China. Soil Tillage Res. 112 (2), 159–166.
Pennell, K.D., 2002. Specific surface area. In: Dane, J.H., Topp, C.G. (Eds.), Methods of Soil Analysis: Part 4 Physical Methods. SSSA Book Series. Soil Science Society of America, Madison, WI, pp. 295–315.
Pires, L.F., Borges, J.A.R., Rosa, J.A., Cooper, M., Heck, R.J., Passoni, S., Roque, W.L., 2017. Soil structure changes induced by tillage systems. Soil Tillage Res. 165, 66–79.
Randolph, P., Bansode, R.R., Hassan, O.A., Rehrah, D., Ravella, R., Reddy, M.R., Watts, D.W., Novak, J.M., Ahmedna, M., 2017. Effect of biochars produced from solid organic municipal waste on soil quality parameters. J. Environ. Manag. 192, 271–280.
Rolston, D., Moldrup, P., 2002. Gas diffusivity. In: Dane, J.H., Topp, G.C. (Eds.), Methods of Soil Analysis. Part 4. SSSA Book Series 5. SSSA, Madison, WI.
Roth, C.H., Pavan, M.A., 1991. Effects of lime and gypsum on clay dispersion and infiltration in samples of a Brazilian Oxisol. Geoderma 48 (3), 351–361.
Schjønning, P., 1985. A Laboratory Method for Determination of Gas Diffusion in Soil. (In Danish with English Summary) Rep. S1773. Danish Inst. of Plant and Soil Sci, Tjele.
Schjønning, P., 1992. Size distribution of dispersed and aggregated particles and of soil pores in 12 Danish soils. Acta Agric. Scand. Sect. B Soil Plant Sci. 42 (1), 26–33.
Schjønning, P., Koppelgaard, M., 2017. The Forchheimer Approach for Soil Air Permeability Measurement. SSSA.
Schjønning, P., Munkholm, L.J., Moldrup, P., Jacobsen, O.H., 2002. Modelling soil pore characteristics from measurements of air exchange: the long-term effects of fertilization and crop rotation. Eur. J. Soil Sci. 53 (2), 331–339.
Schjønning, P., Thomsen, I.K., Møberg, J.P., de Jonge, H., Kristensen, K., Christensen, B.T., 1999. Turnover of organic matter in differently textured soils: I. Physical characteristics of structurally disturbed and intact soils. Geoderma 89 (3–4), 177–198.
Schjønning, P., Thomsen, I.K., Petersen, S.O., Kristensen, K., 2006. Pore Size Distribution, Gas Diffusivity, and Net Nitrogen Mineralization for Soils Under Shallow Tillage and Mouldboard Ploughing. 110–116.
Schjønning, P., Thomsen, I.K., Petersen, S.O., Kristensen, K., Christensen, B.T., 2011. Relating soil microbial activity to water content and tillage-induced differences in soil structure. Geoderma 163 (3–4), 256–264.
Schofield, R.K., 1935. The pF of the water in soil. In: Trans. World Congr. Soil Sci., 3rd, Oxford, UK, (2, 37).
Stepniewski, W., 1981. Oxygen diffusion and strength as related to soil compaction, II oxygen diffusion coefficient. Pol. J. Soil Sci. 14, 11.
Sun, Z., Arthur, E., de Jonge, L.W., Elsgaard, L., Moldrup, P., 2015. Pore structure characteristics after 2 years of biochar application to a sandy loam field. Soil Sci. 180 (2), 41–46.
Sun, Z., Moldrup, P., Elsgaard, L., Arthur, E., Bruun, E.W., Hauggaard-Nielsen, H., de Jonge, L.W., 2013. Direct and indirect short-term effects of biochar on physical characteristics of an arable sandy loam. Soil Sci. 178 (9), 465–473.
Targulian, V.O., Krasilnikov, P.V., 2007. Soil system and pedogenic processes: self-organization, time scales, and environmental significance. Catena 71 (3), 373–381.
Taylor, S.A., 1950. Oxygen diffusion in porous media as a measure of soil aeration. Proc. Soil Sci. Soc. Am. 1949 (14), 55–61.
Thomas, G.W., 1996. Soil pH and soil acidity. In: Sparks, D.L., Page, A.L., Helmke, P.A., Loeppert, R.H. (Eds.), Methods of Soil Analysis. Part 3. Chemical Methods. SSSA, Madison WI.
Thorbjorn, A., Moldrup, P., Blendstrup, H., Komatsu, T., Rolston, D., 2008. A gas diffusivity model based on air-, solid-, and water-phase resistance in variably saturated soil. Vadose Zone J. 7, 1276.
Timmermann, E.O., 2003. Multilayer sorption parameters: BET or GAB values? Colloids Surf. A 220 (1–3), 235–260.
Ulyett, J., Sakrabani, R., Kibblewhite, M., Hann, M., 2014. Impact of biochar addition on water retention, nitrification and carbon dioxide evolution from two sandy loam soils. Eur. J. Soil Sci. 65 (1), 96–104.
Wong, J.T.F., Chen, Z.K., Ng, C.W.W., Wong, M.H., 2016. Gas permeability of biochar-amended clay: potential alternative landfill final cover material. Environ. Sci. Pollut. Res. Int. 23, 7126–7131.
Zhang, M., Cheng, G., Feng, H., Sun, B., Zhao, Y., Chen, H., Chen, J., Dyck, M., Wang, X., Zhang, J., Zhang, A., 2017. Effects of straw and biochar amendments on aggregate stability, soil organic carbon, and enzyme activities in the Loess Plateau, China. Environ. Sci. Pollut. Res. Int. 24, 10108–10120.
Zhu, L., Xiao, Q., Shen, Y., Li, S., 2017. Effects of biochar and maize straw on the short-term carbon and nitrogen dynamics in a cultivated silty loam in China. Environ. Sci. Pollut. Res. 24 (1), 1019–1029.